Langmuir

ARTICLE

pubs.acs.org/Langmuir

Capillary Extraction

Keyvan Piroird,[†,‡] Christophe Clanet,[†,‡] and David Quéré*[,†,‡]

[†]Physique et Mécanique des Milieux Hétérogènes (PMMH), UMR 7636 du CNRS, École Supérieure de Physique et de Chimie Industrielles de la Ville de Paris (ESPCI), 75005 Paris, France

[‡]Ladhyx, UMR 7646 du CNRS, École Polytechnique, 91128 Palaiseau, France

Supporting Information

ABSTRACT: A nonwetting slug placed at the end of a capillary tube is unstable: a small displacement results in the complete extraction of the liquid from the tube. We study two limiting cases, corresponding to a slug viscosity larger or smaller than that of the surrounding liquid. By varying parameters such as the drop and tube length, we identify in each case the dominant dissipation and describe experimentally and theoretically the dynamics of extraction.

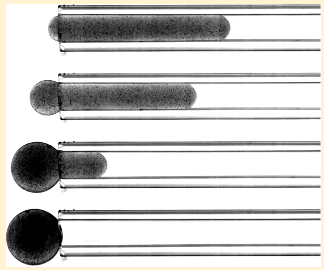

INTRODUCTION

The penetration of a wetting liquid in a capillary tube is a classical problem, at the origin of the science of surface phenomena.[1] Beyond static questions (height of the rise if the tube is vertical, criterion of penetration), researchers described the dynamics of the process.[2,3] For an infinite liquid reservoir, this dynamics was shown to result most often from a balance between surface tension and viscous resistance (proportional to the length of liquid inside the tube). As a consequence, the length of the column increases as the square root of time, which is often referred to as the Lucas−Washburn law.[2,3] At short time, deviations to this law were established and shown to be due to inertia.[4−6] In vertical tubes, deviations have also been observed at long time due to gravity.[3,7] Other deviations arise from the additional dissipation associated with the motion of a contact line at the top of the moving column.[5,8]

Marmur extended the description to the case where the reservoir is a drop of finite radius R. He showed that complete penetration can be achieved in a microgravity environment for contact angles smaller than $\theta_c = 114°$ (instead of 90°, normally), provided that the reservoir drops are smaller than a critical radius $R_c = -R_o/(\cos \theta_c)$, R_o denoting the tube radius.[9] This facilitated wicking is due to the additional Laplace pressure inside the drop, inversely proportional to R. The same phenomenon was studied recently using theory and molecular dynamics simulations in the context of metallic liquid droplets and carbon nanotubes[10] and experimentally with water and PTFE capillary tubes.[11]

In our experiment, the liquid is in a completely nonwetting state ($\theta_c = 180°$) for which adhesion and friction forces are minimized.[12−14] Contrasting with wicking, surface forces are then able to extract liquid from a capillary tube, as shown in Figure 1. An oil slug initially placed at the end of the tube is observed to be unstable and to come out of it. The slug velocity first slowly increases and then reaches a constant value on the order of 1 mm/s. The motion stops when the drop is fully extracted—at the exit of the tube—for our matched-density liquids (last image in Figure 1). The origin of motion can be easily understood: once a meniscus is out of the tube, any further displacement of the slug toward this meniscus reduces the surface energy of the system until the shape of minimum surface, i.e., a sphere is achieved. This phenomenon is analogous to foam coarsening, where small bubbles empty into larger ones due to surface tension.[15] Capillary extraction has been observed in the context of detergency of oil in tubes, where it enables the complete removal of the oil at the end of the experiment.[16] Extraction also exists in the context of cell aggregates manipulated with a micropipet, and it was used to characterize the mechanical properties of those aggregates.[17]

EXPERIMENTAL SECTION

As in Figure 1, a nonwetting slug of silicone oil (poly(dimethylsiloxane), trimethylsiloxy-terminated, CAS number 63148-62-9, provided by ABCR GmbH) of typical viscosity $\eta_o \approx 1$ Pa·s (molar mass 30 000 g/mol) is placed in a capillary tube (borosilicate glass, purchased from Fischer Scientific) of radius $R_o = 0.88$ mm and length $L_t = 40$ mm. The whole device is immersed in a bath of water−ethanol mixture of viscosity $\eta \approx 1$ mPa·s. The bath is prepared by mixing 75% (by weight) water, purified with a Barnstead Easypure II system (the typical conductiviy is 18 MΩ·cm), and 25% ethanol (96%, purchased from Fischer Scientific). To match the densities of both liquids (common density of 960 kg/m^3), exact proportions are adjusted according to the rise or fall of oil in the bath. The surface tension γ between oil and the water−ethanol mixture is 20 ± 2 mN/m, as determined by the pendant drop method, with two different water−ethanol mixtures of densities slightly higher and lower than that of the oil.

Received: April 22, 2011
Revised: June 9, 2011
Published: June 11, 2011

   dx.doi.org/10.1021/la201490m | Langmuir 2011, 27, 9396–9402

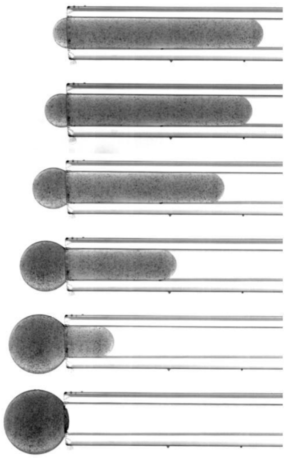

Figure 1. Capillary extraction of a nonwetting oil drop (of viscosity $\eta_o = 1$ Pa·s and density ρ = 960 kg/m^{-3}) initially placed in a glass tube of radius R_o = 0.88 mm and length L_t = 40 mm, fully immersed in a mixture of water and ethanol of the same density: when the drop is placed at the end of the tube, a slight perturbation results in its complete extraction. The movement is accelerated until the slug reaches a constant velocity. The interval between images is 2.5 s.

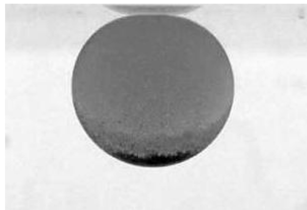

Figure 2. Photograph of an oil drop of radius 2 mm on a treated glass plate immersed in pure water, taken 40 min after first "contact". It is observed that the contact angle remains fixed at its maximum value of 180°.

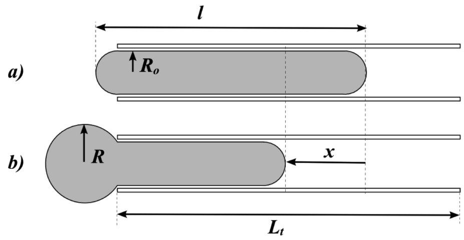

Figure 3. Sketch of the experiment. (a) represents the unstable initial position, as the left end of the slug is out of the tube by a distance equal to the tube radius R_o. (b) Any positive displacement x is amplified until the slug is completely extracted. R is the radius of the outer spherical cap, x is the distance traveled by the other end of the slug, l is the initial length of the slug, and L_t is the length of the tube.

The tube is open at both ends, and it is horizontal, so that hydrostatic pressure is constant. The nonwetting situation is achieved by rubbing the inside of the tube with a polishing powder mainly composed of cerium oxide (Cerox 1650, Rhodia) of typical particle radius 1 μm and then treating it with a 1 M sodium hydroxide solution for 10 min, before rinsing it with purified water. After this treatment, the tube is highly hydrophilic: the contact angle of oil in water (or in water−ethanol mixtures) is observed to be 180°, which implies that a thin lubricating layer of aqueous solution always remains between the oil and the tube. This film does not dewet the surface on the time scale of the experiment, which prevents the formation of a contact line and any hysteresis that may arise from it. We checked that an oil drop on a treated glass in water maintains a contact angle of 180° for at least 40 min (Figure 2).

After insertion of an oil slug of length l into the tube with a syringe, we move it toward the tube end by injecting the water−ethanol mixture at a velocity of 0.1 mm/s. The motion is stopped when the slug extremity is out by a tube radius R_o, as seen in the first image of Figure 1 and in Figure 3a. This position is unstable: if the slug is still pushed by a small distance x ($x \ll R_o$), it spontaneously leaves the tube. The motion is recorded with a Phantom V7.3 camera using a Sigma 50 mm F2.8 DG EX macrolens.

THEORETICAL BASIS

The liquid outside becomes a spherical cap of radius $R > R_o$, connected to a slug of radius R_o ended by a hemisphere of radius R_o, as seen in Figure 1 and sketched in Figure 3b. Such a shape is not an equilibrium shape, owing to the difference of curvature between its ends. A Laplace pressure difference $\Delta P = 2\gamma(1/R_o - 1/R)$ is set between the drop extremities, which induces a flow from the small to the large cap. An initial perturbation x therefore grows until the drop is completely extracted from the tube ($x \simeq l - R_o$).

The driving force arising from the Laplace pressure difference can be written as

$$F(x) = 2\pi\gamma R_o\left(1 - \frac{R_o}{R(x)}\right) \tag{1}$$

Hence, it is not constant during extraction. It starts from a very small value at the onset of movement ($R(x) \gtrsim R_o$), and it continuously increases as the drop comes out. In the limit of very large outer spherical caps ($R(x) \gg R_o$), the force becomes independent of x and equal to its maximum value $2\pi\gamma R_o$. Between these two limits, we need to know how R varies with x to estimate $F(x)$, which is done using conservation of volume.

The initial slug is sketched in Figure 3a: it is composed of a central cylindrical part ended by two hemispherical caps. We work in the limit of large aspect ratio ($l/R_o \gg 1$). During extraction (Figure 3b), the drop consists of the same cylinder reduced by a distance x of one hemisphere of radius R_o and of a spherical cap of volume $V_{cap} = \pi R_o^2 x + 2\pi R_o^3/3$. Since this cap is a sphere of radius R and width $R + (R^2 - R_o^2)^{1/2}$, we get a cubic equation for $R(x)$:

$$(8R_o^3 + 12R_o^2 x)R^3 - 3R_o^4 R^2 - (5R_o^6 + 9R_o^4 x^2 + 12R_o^5 x) = 0 \tag{2}$$

This equation has one real root, whose analytical expression can be found using Cardano's method:

$$R(x) = \frac{R_o^2}{8R_o + 12x} + \left(\frac{R_o^6}{64(2R_o + 3x)^3} - \frac{R_o^2(5R_o^2 + 12R_o x + 9x^2)}{32R_o + 48x}\left(-2 + 3\sqrt{\frac{(3R_o^2 + 8R_o x + 6x^2)^2}{(2R_o + 3x)^2(5R_o^2 + 12R_o x + 9x^2)}}\right)\right)^{1/3}$$
$$+ \left(\frac{R_o^6}{64(2R_o + 3x)^3} + \frac{R_o^2(5R_o^2 + 12R_o x + 9x^2)}{32R_o + 48x}\left(2 + 3\sqrt{\frac{(3R_o^2 + 8R_o x + 6x^2)^2}{(2R_o + 3x)^2(5R_o^2 + 12R_o x + 9x^2)}}\right)\right)^{1/3} \tag{3}$$

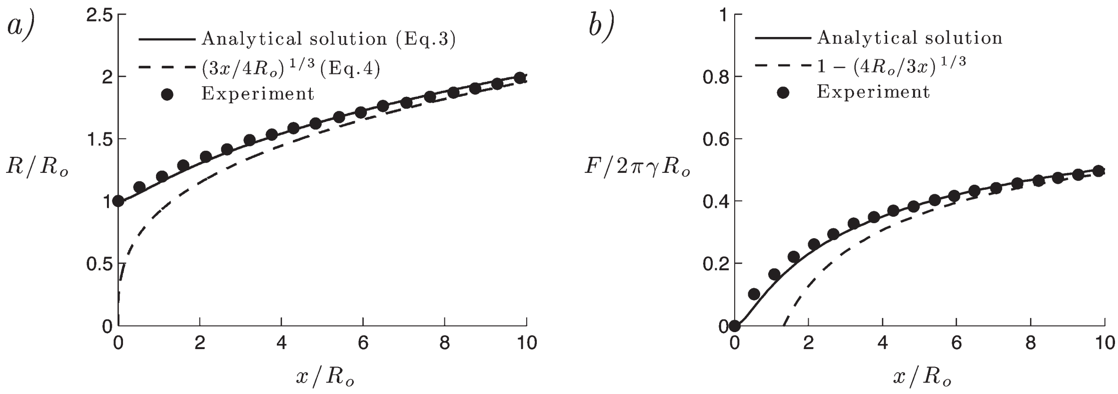

Figure 4. (a) Radius of the outer spherical cap R normalized by the tube radius R_o as a function of the normalized displacement x/R_o. The solid line is the analytical solution from conservation of volume (eq 3), the dotted line is the simplified solution (eq 4), and the circles are data from an extraction experiment similar to that in Figure 1. The simplified expression for R is a good approximation for $x/R_o > 5$. (b) Corresponding driving force $F = 2\pi\gamma R_o(1 - R_o/R)$ normalized by its maximal value expected for $x \gg R_o$. For $x/R_o = 10$, the force is only half its maximal value.

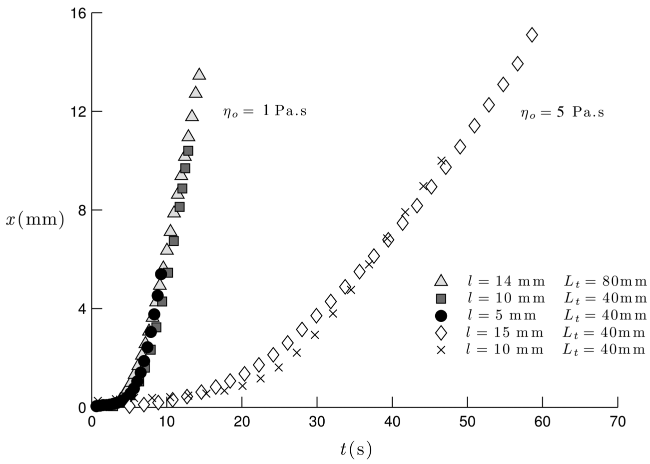

Figure 5. Position of the moving end of the slug as a function of time for various oil viscosities η_o, slug lengths l, and tube lengths L_t in a microgravity environment. The tube radius $R_o = 0.88$ mm. The velocity is almost zero at the beginning, and it tends toward a constant value as the motion proceeds. This value is lower for high viscosities, and the general shape of this curve does not seem to depend on the length of the slug nor on the tube length. The origin of time is chosen a few seconds before the movement of the slug becomes measurable.

In the limit $x \gg R_o$, this expression simplifies to

$$R(x) \simeq \left(\frac{3}{4}R_o{}^2x\right)^{1/3} \tag{4}$$

This equation just expresses the conservation of volume between a cylinder of radius R_o and length x and a sphere of radius R. To study the transition from eq 3 to its limit (eq 4), we have conducted experiments similar to the one shown in Figure 1, and we present in Figure 4a the evolution of the ratio R/R_o as a function of the reduced extraction distance x/R_o.

We verify the accuracy of the analytical expression (eq 3) and observe that the approximation (eq 4) only approaches the experimental data when x/R_o becomes larger than 5. For larger x, the ratio R_o/R decreases slowly, as $(R_o/x)^{1/3}$. This implies that the constant force limit is slowly approached and that we have to take into account the full expression for $R(x)$ if we want to describe accurately the extraction. This is emphasized in Figure 4b: for $x/R_o = 10$, the force is only equal to half its maximal value expected for $x/R_o \gg 1$. In fact, x/R_o has to be equal to 1000 to have a force equal to 90% of its maximal value.

RESULTS AND DISCUSSION

Dynamics. The extraction dynamics is shown in Figure 5 for various viscosities, slug lengths, and tube lengths. The tube radius is $R_o = 0.88$ mm, and $x = 0$ corresponds to the unstable position (first image in Figure 1). The position x of the right end of the slug increases more and more rapidly as time goes on: the slug velocity is almost zero at the beginning, and it tends toward a constant at the end. The dynamics is not affected when the initial drop length l is modified by a factor of 3 nor when the tube length L_t is changed by a factor of 2. We can also notice that extraction takes approximately 10 s for a slug of viscosity $\eta_o \approx 1$ Pa·s and length $l = 10$ mm, instead of 50 s if we increase η_o by a factor of 5, keeping the other parameters constant.

To account for these observations, we have to identify the sources of dissipation in this system. Since the Reynolds number is always very small (for a velocity $V \approx 1$ mm/s, $Re_o = \rho V R_o/\eta_o$ in oil is smaller than 10^{-3}, and $Re_w = \rho V R_o/\eta$ in water−ethanol is smaller than 1), inertia can be neglected. Moreover, the viscosity ratio η_o/η is on the order of 1000, so that we can ignore the dissipation due to the flow of the water−ethanol mixture in the tube, as confirmed by the fact that the dynamics is not modified by doubling the length L_t. Thus, the dominant viscous dissipation can a priori be in the oil or in the lubricating layer.

To evaluate the dissipation in oil, we need to characterize the flow profile in the slug. In the presence of an aqueous lubricating layer 1000 times less viscous than oil, we might expect a plug flow in the oil. This can be checked experimentally by injecting small tracer particles into the slug and following their displacement using a long-exposure photograph, as shown in Figure 6a and 6b. From this picture, we can deduce the velocity profile $v(r)$ in the slug, as displayed in Figure 6b. The lens used to record this experience has a shallow depth-of-field (<1 mm), which allows us to track only the particles in the plane containing the axis of symmetry of the tube and perpendicular to the optical axis. The profile is clearly not a Poiseuille flow. The velocity slowly decays with r: it is equal to 0.15 ± 0.02 mm/s on the center line and to 0.13 ± 0.02 mm/s near the tube wall, i.e., roughly 10% slower than at the center.

This observation contrasts with what we observe at the exit of the tube: as seen in the bottom picture of Figures 6a and 6b, the

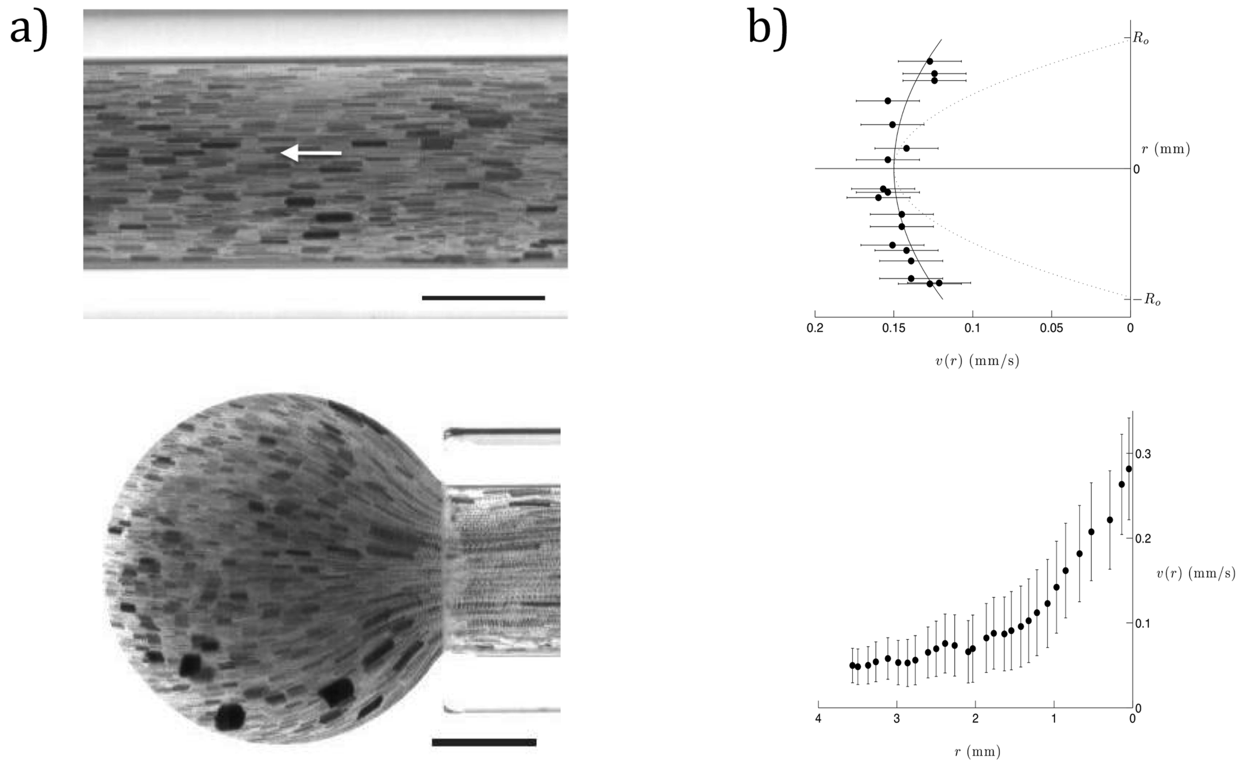

Figure 6. (a) Long-exposure photograph in an oil slug of viscosity η_o = 5 Pa·s moving in a tube of radius R_o = 0.88 mm. The oil contains small tracers, which yields an estimate of the velocity profile. The exposure time is 2 s, and the bar represents 1 mm in both photographs. The top image is a close-up view in the middle of the slug: the flow is very similar to a plug flow. The direction of the motion is indicated by the white arrow. The bottom image is taken at the exit. The velocity decays over a distance comparable to the tube radius. (b) Velocity profile extracted from (a). The profile in the middle of the slug is clearly not a Poiseuille flow (drawn with a dotted line), which confirms the presence of a lubricating film. The solid line is the equation $v(r)$ (mm/s) = 0.15 − 0.04r^2. At the exit of the tube (r is the distance from this exit), the velocity drops on a distance of order R_o.

oil velocity decreases at a distance on the order of R_o. The Laplacian of the velocity is therefore on the order of $\dot{x}/R_o^2$, and the typical volume in which the flow occurs is R_o^3. We therefore expect a dissipative force scaling as $\eta_o \dot{x} R_o$ (very different from the viscous force opposing the rise of liquid in a tube, which is proportional to the height of the column). More precisely, Sampson showed that the pressure drop due to the flow from an infinite reservoir through an orifice of radius R_o is $\Delta P = 3\pi\eta_o V/R_o$, with V the mean flow velocity.[18] The viscous force thus scales as $F = 3\pi^2\eta_o V R_o$. Johansen experimentally investigated this problem and found similar results, with a small corrective term $(1 - (R_o/R)^4)$ to take into account the finite size R of the reservoir.[19]

Another source of dissipation arises from the shear stress in the lubricating film. It generates a viscous resistance scaling as $2\pi\eta(\dot{x}/h)(l - x)R_o$, where h is the thickness of the film. We can estimate this thickness from the observation that the velocity profile in the oil does not deviate from a plug flow by more than roughly 10%. Using the stress continuity at the oil/water interface, we find

$$\eta \frac{V_{int}}{h} \approx \eta_o \frac{V - V_{int}}{R_o} \tag{5}$$

where V is the maximal fluid velocity in the slug and V_{int} is the velocity at the oil/water interface. Assuming $V_{int} = 0.90 \pm 0.05$ V, we obtain

$$h \approx 10 R_o \frac{\eta}{\eta_o} \approx 10\ \mu\text{m} \tag{6}$$

We can now compare the dissipative forces in the film and in the oil. The dissipation in the oil cap will be dominant if we have

$$2\pi\eta \frac{V}{h} R_o(l - x) < 3\pi^2\eta_o V R_o \tag{7}$$

which gives

$$l - x < \frac{3\pi}{2}\frac{\eta_o}{\eta} h \approx 50 R_o \tag{8}$$

The dissipation in oil is therefore always dominant during the last phase of the movement, when the slug distance to the exit is less than approximately $50R_o$. We worked with slug lengths between $5R_o$ and $17R_o$, meaning that the dissipation in the film is negligible. In this limit, the force balance on the slug can be written as

$$2\pi\gamma R_o\left(1 - \frac{R_o}{R(x)}\right) = 3\pi^2\eta_o R_o \dot{x} \tag{9}$$

This differential equation can be solved numerically by using the analytical result for $R(x)$ (eq 3), as shown in Figure 7. The equation depends neither on l nor on L_t, in accord with the experiments. It also gives a "final" constant velocity for the slug, which is equal to

$$V = \frac{2}{3\pi}\frac{\gamma}{\eta_o} \tag{10}$$

This quantity is inversely proportional to the oil viscosity η_o, as suggested in Figure 5. In the dimensionless coordinates x/R_o,

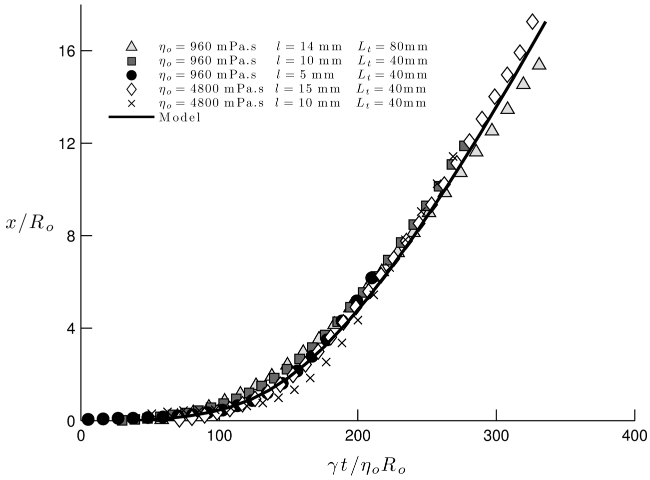

Figure 7. Position of the trailing end of the slug normalized by the tube radius as a function of dimensionless time $\gamma t/\eta_o R_o$. The symbols and data are the same as in Figure 5. The solid line is the solution of eq 9 with a prefactor of 0.18 (close to $2/3\pi \approx 0.21$).

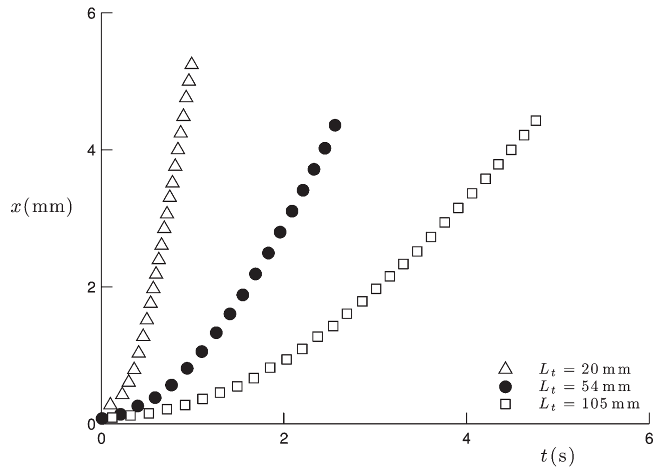

Figure 8. Position of the trailing edge of an air slug, initially placed at the exit of a tube of radius R_o = 0.3 mm, as a function of time for three different tube lengths L_t. The slug length is the same in the three experiments ($l \approx$ 5 mm). The surrounding liquid is silicone oil of viscosity η = 4.5 mPa·s.

$\gamma t/\eta_o R_o$, the data collapse on a master curve, which is itself well described by the solution of eq 8 drawn with a solid line. The prefactor taken for the fit is 0.18, close to the expected value $2/3\pi \approx 0.21$.

We can finally notice that the velocity approaches a constant value, as seen in the data. However, the value observed in Figure 7 for the largest x/R_o is only half the maximal predicted value $2\gamma/3\pi\eta_o$ because of the slow decay of the quantity R_o/R (which is still 0.43 for x/R_o = 16).

Air Slug. We also investigated the opposite limit where the viscosity ratio η_o/η is small compared to 1. The slug is now an air bubble, and the bath is filled with silicone oil of viscosity η = 4.5 mPa·s (200 times more viscous than air) that completely wets the tube. Since the microgravity condition cannot be fulfilled anymore, the air slug is likely to be cut in several pieces during extraction, unless the tube is small enough. This problem is similar to the question of the maximal volume of a drop hanging from a cylindrical nozzle of radius R_o.[20] Balancing the weight (or buoyancy in our case) $\Delta\rho g R^3$ (where $\Delta\rho$ is the density difference between the two fluids) with the surface force γR_o, we find that the slug breaks if its volume is larger than $a^2 R_o$, where $a = (\gamma/\Delta\rho g)^{1/2} \approx 1.5$ mm is the capillary length of silicone oil (with γ = 20 mN/m and $\Delta\rho$ = 915 kg/m^3). In other terms, the slug will be extracted in one piece if we have

$$R_o l < a^2 \tag{11}$$

For a slug length l = 5 mm, this yields a critical tube radius $R_o^* \approx \gamma/\Delta\rho g l \approx 0.4$ mm below which gravity effects can be neglected.

In Figure 8, we observe the position of the trailing edge of the air slug as it gets extracted out of a tube of radius R_o = 0.3 mm. The driving force is the same as before (eq 1), but the dissipation is different, as revealed by the data. The dynamics is slower if the tube is longer: it takes 1 s to extract an air slug of length l = 5 mm from a tube of length L_t = 20 mm, whereas it takes about 5 s for the same slug placed in a tube 5 times longer (L_t = 105 mm).

The observations indicate that the flow of oil behind the slug must be taken into account in the limit where the slug viscosity becomes negligible compared to that of the surrounding liquid.

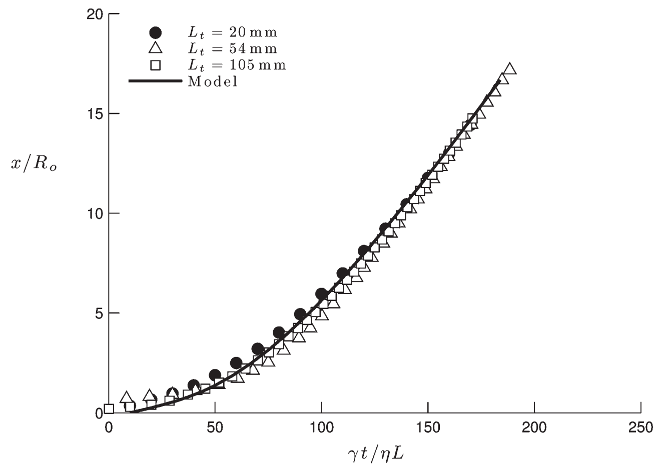

Figure 9. Position of the trailing edge of an air slug as a function of time for three different tube lengths. The slug length is kept constant ($l \approx$ 5 mm), and R_o = 0.3 mm. The data of Figure 8 are compared with solution of eq 13 (with a prefactor of 0.25), drawn with a solid line.

Since the Reynolds number is always smaller than 0.1, we assume a Poiseuille flow in the tube. Balancing the driving force by the dissipation arising from such a flow gives

$$2\pi\gamma R_o\left(1 - \frac{R_o}{R(x)}\right) = 8\pi\eta\dot{x}(L_t - l + x) \tag{12}$$

The viscous resistance now depends on L_t and increases linearly with x. However, since $L_t \gg l$, the variation is always small (roughly 10% of its initial value) compared to the variation of the driving force, which varies between 0 and $2\pi\gamma R_o$. Hence, we can approximate the right-hand term by $8\pi\eta\dot{x}L_t$. This yields the following differential equation:

$$\frac{\dot{x}}{R_o} = \frac{\gamma}{4\eta L_t}\left(1 - \frac{R_o}{R(x)}\right) \tag{13}$$

Hence, we expect a maximal velocity equal to $\gamma R_o/4\eta L_t$, which depends on the tube aspect ratio R_o/L_t. We deduce from eq 13 a new dimensionless expression for time ($\gamma t/\eta L_t$), allowing us to

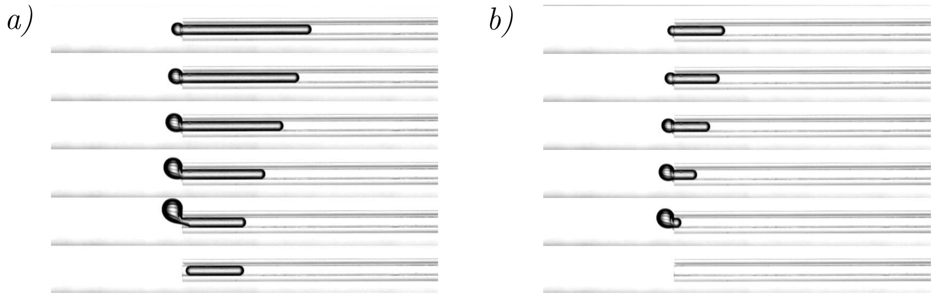

Figure 10. Effect of gravity on the extraction of an air slug of length l from a capillary tube of radius R_o = 0.3 mm and total length L_t = 52 mm. (a) l = 8.5 mm: the slug breaks into two parts, a bubble (of radius 0.65 mm) escapes from the tube, and the other part (of length 3.4 mm) remains trapped inside the tube. (b) l = 3.4 mm: the slug is fully extracted without breaking, in agreement with eq 11.

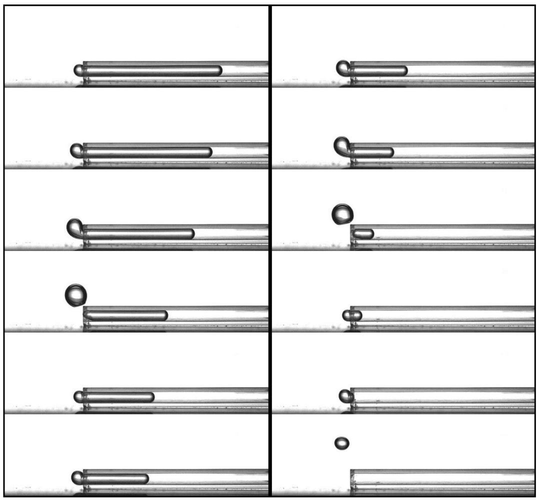

Figure 11. Extraction of an air slug (of initial length l = 23 mm) from a tube of radius R_o = 0.88 mm and length L_t = 40 mm. Gravity cuts the air slug in two, but the remaining part keeps a small velocity (probably due to inertia), allowing it to move to the exit of the tube. A new extraction process starts, and the slug eventually gets fully extracted.

collapse the data of Figure 8 on a master curve shown in Figure 9. The model (eq 13) is in good agreement with the data without any adjustable parameter.

In this case again, the velocity slowly tends to its maximal value because of the weak dependence of the driving force on x. The maximal slope in Figure 9 is still only half of $\gamma R_o/4\eta L_t$ for $x/R_o \approx 16$.

Gravity Effects. We finally look at the limit where gravity effects cannot be neglected. According to eq 11, gravity breaks slugs of length l larger than a^2/R_o = 7.5 mm for R_o = 0.3 mm. Figure 10 shows two extraction experiments made in a tube of radius R_o = 0.3 mm and length L_t = 52 mm with two different slug lengths. In Figure 10a where l = 8.5 mm, the air slug is cut into two parts: a bubble of radius 0.65 mm that escapes and a remaining slug of length 3.4 mm. This remaining slug has no further reason to move: its left end is entirely inside the tube and distant from the unstable position by at least R_o (last picture of Figure 10a). In Figure 10b, it is observed that a shorter slug, of initial length l = 3.4 mm, is able to escape entirely without breaking. No air is left inside the tube at the end of the experiment.

In case a, the force balance between buoyancy and capillarity predicts a rising bubble of radius $R^* \approx (a^2R_o)^{1/3}$ = 0.88 mm, on the order (yet slightly larger, like in Tate's law[20]) of 0.65 mm measured in Figure 10a. As discussed in eq 11, gravity imposes an upper bound to the maximal volume a^2R_o that can be extracted, which is a serious limitation for potential applications. However, in bigger tubes (R_o = 0.88 mm, L_t = 40 mm), it is observed that after pinch-off, the remaining part still has a small velocity, probably due to inertia (the Reynolds number just before the first pinch-off is ~1), which is enough to bring it to the unstable position, as seen in Figure 11 between the third and fourth pictures. The extraction process can start again, and so on, until no air is left inside the tube. In Figure 11, the air slug is completely extracted after the second pinch-off.

■ CONCLUSION

We discussed capillary extraction, which is the process by which a nonwetting liquid spontaneously leaves a capillary tube owing to surface tension. In contrast with wicking, extraction is observed for liquids with a high contact angle (close to 180°), and it follows a very different dynamics: the velocity slowly increases from zero to a constant value.

As a first reason for this difference, the driving force is not constant: it is infinitesimally small at the onset of movement, and it slowly tends to a constant value as the slug comes out. Second, the dissipation in our system is also different: due to the presence of a lubricating layer between the slug and the tube, the flow profile in the oil is not a Poiseuille flow as in capillary rise but a plug flow, so that the dissipation at the exit of the tube becomes the main source of resistance if the oil is viscous.

We discussed quantitatively the origin of the viscous resistance in this limit from which we deduced the extraction velocity. We also investigated the opposite limit of an air slug of viscosity much smaller than that of the surrounding liquid and showed that the dynamics is controlled by the viscous dissipation in the liquid behind the slug.

Finally, we qualitatively studied the case where gravity effects are not negligible. They tend to break the slug in parts which can be a limiting factor for the total volume extracted at very low Reynolds numbers. However, for Reynolds number close to 1 (millimetric tubes), the slug remaining in the tube still keeps a small velocity, leading to a new extraction process, and so on, until complete oil extraction.

■ ASSOCIATED CONTENT

S Supporting Information. Two movies showing extraction phenomena, corresponding to Figures 1 and 11. This material is available free of charge via the Internet at http://pubs.acs.org/

AUTHOR INFORMATION

Corresponding Author
*E-mail: david.quere@espci.fr.

REFERENCES

(1) Laplace, P.-S. *Traité de Mécanique Céleste*; Éditions J. Gabay: Paris, 1843.
(2) Lucas, R. *Kolloid-Z.* **1918**, *23*, 15–22.
(3) Washburn, E. W. *Phys. Rev.* **1921**, *17*, 273–283.
(4) Quéré, D. *Europhys. Lett.* **1997**, *39*, 533–538.
(5) Lavi, B.; Marmur, A.; Bachmann, J. *Langmuir* **2008**, *24*, 1918–1923.
(6) Fries, N.; Dreyer, M. *J. Colloid Interface Sci.* **2008**, *327*, 125–128.
(7) Fries, N.; Dreyer, M. *J. Colloid Interface Sci.* **2008**, *320*, 259–263.
(8) Hamraoui, A.; Thuresson, K.; Nylander, T.; Yaminsky, V. *J. Colloid Interface Sci.* **2000**, *226*, 199–204.
(9) Marmur, A. *J. Colloid Interface Sci.* **1988**, *122*, 209–219.
(10) Schebarchov, D.; Hendy, S. C. *Phys. Rev. E* **2008**, *78*, 046309.
(11) Willmott, G. R.; Neto, C.; Hendy, S. C. *Faraday Discuss.* **2010**, *146*, 233–245.
(12) Mahadevan, L.; Pomeau, Y. *Phys. Fluids* **1999**, *11*, 2449–2453.
(13) Yoshimitsu, Z.; Nakajima, A.; Watanabe, T.; Hashimoto, K. *Langmuir* **2002**, *18*, 5818–5822.
(14) Reyssat, M.; Richard, D.; Clanet, C.; Quéré, D. *Faraday Discuss.* **2010**, *146*, 19–33.
(15) Durian, D. J.; Weitz, D. A.; Pine, D. J. *Phys. Rev. A* **1991**, *44*, 7902–7905.
(16) Piroird, K; Clanet, C.; Quéré, D. *Soft Matter* **2011**, DOI: 10.1039/c1sm05282a.
(17) Guevorkian, K.; Colbert, M.-J.; Durth, M.; Dufour, S.; Brochard-Wyart, F. *Phys. Rev. Lett.* **2010**, *104*, 218101.
(18) Sampson, R. A. *Philos. Trans. R. Soc., A* **1891**, *182*, 449–518.
(19) Johansen, F. C. *Proc. R. Soc. London, A* **1930**, *126*, 231–245.
(20) Tate, T. *Philos. Mag.* **1864**, *27*, 176–180.